Intensity correlations between reflected and transmitted speckle patterns

N. Fayard,[1] A. Cazé,[2] R. Pierrat,[1] and R. Carminati[1,*]

[1]*ESPCI ParisTech, PSL Research University, CNRS, Institut Langevin, 1 rue Jussieu, F-75005 Paris, France*
[2]*Department of Mathematics, University of Michigan, Ann Arbor, Michigan 48109, USA*

We study theoretically the spatial correlations between the intensities measured at the input and output planes of a disordered scattering medium. We show that at large optical thicknesses, a long-range spatial correlation persists and takes negative values. For small optical thicknesses, short-range and long-range correlations coexist, with relative weights that depend on the optical thickness. These results may have direct implications for the control of wave transmission through complex media by wave-front shaping, thus finding applications in sensing, imaging, and information transfer.

I. INTRODUCTION

The study of wave scattering in disordered media is an active field of research, stimulated both by innovative applications in imaging and sensing [1] and by fundamental questions in mesoscopic physics [2]. In the last few years, the possibility to control the propagation of optical waves in complex media in the multiple-scattering regime has been demonstrated using wave-front shaping techniques [3,4]. This breakthrough offers perspectives for imaging and communication through complex media [5–7]. The initial schemes make use of optimization techniques requiring intensity measurements in the transmitted speckle, which in terms of practical applications is a serious drawback. Finding a way to control the transmission and focusing of light through a strongly scattering medium from measurements of the reflected speckle only is an issue of tremendous importance. Progress has been made recently by taking advantage of the memory effect [8–10], with imaging capabilities limited to relatively small optical thicknesses. Nevertheless, the connection between the reflected and the transmitted speckle patterns generated by a disordered medium in the multiple-scattering regime has not been addressed theoretically so far.

In this paper, we make a step in this direction by studying theoretically and numerically the statistical correlation between the intensities measured in the transmitted and the reflected speckle patterns. The spatial intensity correlation function $C(\mathbf{r},\mathbf{r}')$ is defined as

$$C(\mathbf{r},\mathbf{r}') = \frac{\langle \delta I(\mathbf{r}) \delta I(\mathbf{r}') \rangle}{\langle I(\mathbf{r}) \rangle \langle I(\mathbf{r}') \rangle}, \qquad (1)$$

where the notation $\langle \ldots \rangle$ denotes a statistical average over disorder and $\delta I(\mathbf{r}) = I(\mathbf{r}) - \langle I(\mathbf{r}) \rangle$ is the intensity fluctuation. This correlation function has been extensively studied in the context of wave scattering and mesoscopic physics [11–14]. Theoretical approaches often make use of the canonical slab or waveguide geometries (for a review see [11,12,15] and references therein), where either transmitted or reflected intensity is considered, or consider point sources in an infinite or open medium and compute intensity correlations for two points inside or outside the medium [16–20]. It seems that

the intensity correlation function for two points lying on different sides of a slab medium has not been studied and that the existence of a correlation has only been mentioned through passing [21,22]. In this work, we study the correlation between the intensities in the input and output planes of a strongly scattering slab, as sketched in Fig. 1. Using numerical simulations and analytical calculations, we show that for optically thick slabs a correlation persists and takes negative values. Moreover, at smaller optical thicknesses, short- and long-range correlations coexist, with relative weights that depend on the optical thickness. We believe these results to be a step forward for the control of transmission through strongly scattering media, thus finding applications in sensing, imaging, and information transfer.

The spatial intensity correlation in a speckle pattern can be split into three contributions, historically denoted by C_1, C_2, and C_3 [11,23], as follows:

$$C(\mathbf{r},\mathbf{r}') = C_1(\mathbf{r},\mathbf{r}') + C_2(\mathbf{r},\mathbf{r}') + C_3(\mathbf{r},\mathbf{r}'). \qquad (2)$$

The first term C_1 corresponds to the Gaussian statistics approximation for the field amplitude, and is a short-range contribution, whose width determines the average size of a speckle spot [16]. C_2 and C_3 are non-Gaussian long-range correlations that decay on much larger scales [23,24]. In the diffusive regime, and for two observation points lying on the same side of the scattering medium, these three contributions have different weights such that $C_1 \gg C_2 \gg C_3$. In the reflection-transmission configuration considered here, and at large optical thickness, we show that an intensity correlation persists and is dominated by C_2 because of the short-range behavior of C_1. In this case, the long-range character of C_2 is conferred by its algebraic decay with respect to the distance between the two observation points. Moreover, this correlation is negative, a result that may have implications in the context of wave control by wave-front shaping. For smaller optical thicknesses, we also show that a crossover can be found between regimes dominated by C_1 and C_2, respectively.

The paper is organized as follows. In Sec. II, we study the reflection-transmission correlation function at large optical thicknesses. First, we use numerical simulations to compute the correlation function without approximation and to describe its main features. Second, we present the analytical calculation of the C_2 contribution to the reflection-transmission correlation
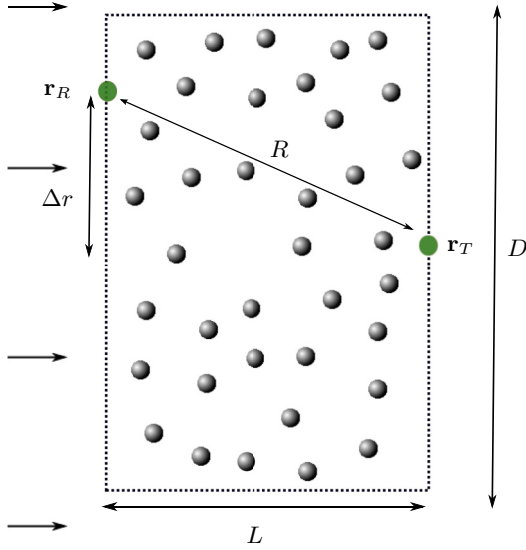
*remi.carminati@espci.fr

FIG. 1. (Color online) Schematic representation of the scattering medium. The slab of thickness L and transverse size D is illuminated from the left by a monochromatic plane wave at normal incidence. The correlation between the reflected and transmitted speckle patterns is characterized by the correlation function between the intensities at points $\mathbf{r}_R$ (reflection) and $\mathbf{r}_T$ (transmission).

function in the multiple-scattering regime, for both two-dimensional (2D) and three-dimensional (3D) geometries, and show that C_2 is the leading contribution at large optical thicknesses. In Sec. III, we study the correlation function at small optical thicknesses, a regime in which the C_1 contribution dominates. In Sec. IV, as a consequence of the negative value of the correlation that is found in the multiple-scattering regime, we describe some peculiarities of the statistical distribution of the product of the reflected and transmitted intensities. Finally, in Sec. V we summarize the main results and discuss some implications for the control of wave transmission through disordered media.

II. REFLECTION–TRANSMISSION CORRELATION AT LARGE OPTICAL THICKNESS

A. Numerical analysis

In this section we present exact numerical simulations of wave scattering in the multiple-scattering regime. We restrict ourselves to a 2D geometry for the sake of computer memory and time. We consider a slab of scattering material, characterized by its thickness L and its transverse size D (we keep $D > 6L$ in order to avoid finite size effects), as depicted in Fig. 1. Our purpose is the calculation of the correlation function $C(\mathbf{r}_R, \mathbf{r}_T)$, where $\mathbf{r}_R$ is a point located on the input surface (reflection) and $\mathbf{r}_T$ is a point located on the output surface (transmission).

1. Method

To proceed, we use the coupled dipoles method [25] to calculate numerically the intensity in the transmitted and reflected speckle patterns. Repeating the calculations for a large number of configurations of disorder (positions of

scatterers) allows us to compute statistics. The system contains N randomly distributed nonoverlapping point scatterers and is illuminated by a plane wave from the left at normal incidence. We deal with TE-polarized waves with an electric field oriented along the invariance axis of the system (scalar waves). The resonant point scatterers are described by their electric polarizability

$$\alpha(\omega) = -\frac{2\Gamma}{k_0^2(\omega - \omega_0 + i\Gamma/2)}, \tag{3}$$

where ω_0 is the resonance frequency and Γ the linewidth. This specific form of the polarizability fulfils the optical theorem (i.e., energy conservation). From the polarizability the scattering cross section $\sigma(\omega) = k_0^3|\alpha(\omega)|^2/4$ and the scattering mean free path $\ell(\omega) = [\rho\sigma(\omega)]^{-1}$ can be deduced, where $\rho = N/(LD)$ is the number density of scatterers. In the following, we consider scatterers at resonance ($\omega = \omega_0$) in order to reach large optical thicknesses with a reasonable number of scatterers (typically a few hundreds). In the coupled dipoles formalism, the exciting field E_j on scatterer number j is written as [25]

$$E_j = E_0(\mathbf{r}_j) + \alpha(\omega)k_0^2 \sum_{\substack{k=1 \\ k \neq j}}^{N} G_0(\mathbf{r}_j - \mathbf{r}_k)E_k, \tag{4}$$

where G_0 is the 2D free-space Green function given by $G_0(\mathbf{r} - \mathbf{r}') = (i/4)\,\mathrm{H}_0^{(1)}(k_0|\mathbf{r} - \mathbf{r}'|)$, $\mathrm{H}_0^{(1)}$ being the Hankel function of first kind and order zero. Equation (4) defines a set of N linear equations that are solved by a standard matrix inversion procedure. Once the exciting field is known on each scatterer, the field $E(\mathbf{r})$ and the intensity $I(\mathbf{r}) = |E(\mathbf{r})|^2$ at any position $\mathbf{r}$ inside or outside the scattering medium can be calculated by a direct summation using

$$E(\mathbf{r}) = E_0(\mathbf{r}) + \alpha(\omega)k_0^2 \sum_{j=1}^{N} G_0(\mathbf{r} - \mathbf{r}_j)E_j. \tag{5}$$

2. Numerical experiment

We have carried out numerical simulations in the multiple-scattering regime with an optical thickness $b = L/\ell = 7$. This choice of optical thickness is limited by the number of configurations that can be calculated in a reasonable computer time in order to get a sufficiently accurate statistics to compute averaged values (requiring typically 10^6 configurations). The correlation function C_{num} obtained from numerical calculation is plotted in Fig. 2 (red solid line) versus the lateral shift Δr between the observation points in the reflected and transmitted speckles (see the geometry in Fig. 1).

Surprisingly, an intensity correlation subsists even for large optical thicknesses (multiple-scattering regime). Moreover, the reflection-transmission correlation function at large optical thickness takes a negative value around $\Delta r = 0$. This means that $\langle \delta I(\mathbf{r}_R)\delta I(\mathbf{r}_T)\rangle < 0$, showing that the probability to have a dark spot in the transmitted speckle in lateral coincidence with a bright spot in the reflection speckle (and *vice versa*) should be substantial. This property, that might have implications for the control of wave transmission by wave-front shaping, is investigated more precisely in Sec. IV.
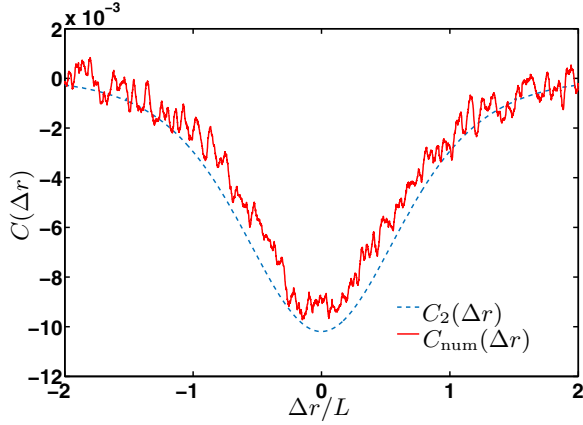
FIG. 2. (Color online) Reflection–transmission intensity correlation C_{num} given by the numerical simulations (red solid line) and analytical correlation C_2 given by Eq. (29) (blue dashed line). Multiple-scattering regime with $b = 7$ and $k_0\ell = 10$.

B. Analytical derivation of the C_2 reflection-transmission correlation function

To get more insight on the numerical result presented above, we present the calculation of the C_2 contribution to the intensity correlation function for scalar waves in both 2D and 3D geometries. Intuitively, we expected C_2 to be the leading contribution at large optical thicknesses, since C_3 is always negligible compared to C_2, and C_1 vanishes exponentially with the optical thickness in this particular reflection-transmission configuration.

For a dilute system such that $k_0\ell \gg 1$, where $k = \omega/c = 2\pi/\lambda$ with c the speed of light and λ the wavelength in vacuum, the intensity correlation functions can be calculated analytically using a perturbative approach. Since the calculation for reflection-reflection or transmission-transmission correlations is detailed in textbooks or review articles [2,11,14], we do not give all the details here but rather focus on the specificity of the reflection-transmission geometry. For the analytical derivation, we consider that the transverse size D of the slab is infinite.

1. Average intensity

To compute the correlation function C_2, we first need to compute the average intensity. The starting point is the Bethe-Salpeter equation that reads [2,14]

$$\langle E(\mathbf{r},\omega)E^*(\mathbf{r}',\omega)\rangle$$
$$= \langle E(\mathbf{r},\omega)\rangle\langle E^*(\mathbf{r}',\omega)\rangle + \int \langle G(\mathbf{r},\mathbf{r}_1,\omega)\rangle\langle G^*(\mathbf{r}',\mathbf{r}_2,\omega)\rangle$$
$$\times \Gamma(\mathbf{r}_1,\mathbf{r}_2,\mathbf{r}_3,\mathbf{r}_4,\omega)\langle E(\mathbf{r}_3,\omega)E^*(\mathbf{r}_4,\omega)\rangle d\mathbf{r}_1 d\mathbf{r}_2 d\mathbf{r}_3 d\mathbf{r}_4. \quad (6)$$

In this equation, $\langle G(\mathbf{r},\mathbf{r}',\omega)\rangle$ is the average Green function that links the average field $\langle E(\mathbf{r},\omega)\rangle$ to a source dipole p located at position $\mathbf{r}'$ via $\langle E(\mathbf{r},\omega)\rangle = \mu_0\omega^2\langle G(\mathbf{r},\mathbf{r}',\omega)\rangle p$. The operator $\Gamma(\mathbf{r}_1,\mathbf{r}_2,\mathbf{r}_3,\mathbf{r}_4,\omega)$ is the irreducible vertex that contains all multiple-scattering sequences connecting $(\mathbf{r}_3, \mathbf{r}_4)$ to $(\mathbf{r}_1, \mathbf{r}_2)$. The exact calculation of this complex object is out of reach, but an approximate expression to first order in the small parameter

$1/(k_0\ell)$ and for independent scattering, known as the ladder approximation, can be derived [14]. Omitting the frequency dependence for simplicity in the following, it reads

$$\Gamma(\mathbf{r}_1,\mathbf{r}_2,\mathbf{r}_3,\mathbf{r}_4) = \gamma\delta(\mathbf{r}_1 - \mathbf{r}_2)\delta(\mathbf{r}_3 - \mathbf{r}_4)\delta(\mathbf{r}_1 - \mathbf{r}_3), \quad (7)$$

where

$$\gamma = \begin{cases} 4k_0/\ell & \text{for 2D TE waves (2D),} \\ 4\pi/\ell & \text{for 3D scalar waves (3D).} \end{cases} \quad (8)$$

Plugging Eq. (7) into Eq. (6) yields

$$\langle I(\mathbf{r})\rangle = \underbrace{|\langle E(\mathbf{r})\rangle|^2}_{I_B(\mathbf{r})} + \underbrace{\gamma \int |\langle G(\mathbf{r},\mathbf{r}')\rangle|^2\langle I(\mathbf{r}')\rangle d\mathbf{r}'}_{I_D(\mathbf{r})}. \quad (9)$$

Physically, this closed equation means that only contributions for which E and E^* follow the same scattering path have a significant weight in the average intensity (all cross terms vanish). The first term I_B in Eq. (9) is the ballistic (or coherent) component of the average intensity and the second term I_D is the diffuse part. In order to get explicit expressions for these two quantities, we need to compute the average Green function, or equivalently, the average field. As a consequence of the Dyson equation [14], in the independent scattering limit, the average Green function obeys a propagation equation in an effective homogeneous medium, defined by an effective wave vector k_{eff}. We have

$$\langle G(\mathbf{r})\rangle = \begin{cases} \frac{i}{4}H_0^{(1)}(k_{eff}|\mathbf{r}|) & \text{(2D),} \\ \frac{\exp(ik_{eff}|\mathbf{r}|)}{4\pi|\mathbf{r}|} & \text{(3D),} \end{cases} \quad (10)$$

and

$$\langle E(\mathbf{r})\rangle = E_0 \exp(ik_{eff}z), \quad (11)$$

where $k_{eff} = k_0 + i/(2\ell)$ to first order in $1/(k_0\ell)$ and z is the coordinate along the direction normal to the slab. The ballistic intensity is readily deduced:

$$I_B(z) = I_0 \exp[-z/\ell]. \quad (12)$$

Regarding the diffuse intensity $I_D(\mathbf{r})$, we can rewrite Eq. (9) in the following way:

$$I_D(\mathbf{r}) = \gamma \int |\langle G(\mathbf{r},\mathbf{r}')\rangle|^2[I_B(\mathbf{r}') + I_D(\mathbf{r}')]d\mathbf{r}'. \quad (13)$$

An analytical expression of the diffuse intensity can be obtained in the diffusive limit where $|\mathbf{r} - \mathbf{r}'| \gg \ell$. Making use of the translational invariance of the medium, the Fourier transform of Eq. (13) reads

$$I_D(\mathbf{q}) = \gamma A(\mathbf{q})[I_B(\mathbf{q}) + I_D(\mathbf{q})], \quad (14)$$

where

$$A(\mathbf{q}) = \frac{1}{\gamma} \times \begin{cases} \frac{1}{\sqrt{1+q^2\ell^2}} & \text{(2D),} \\ \frac{\arctan(q\ell)}{q\ell} & \text{(3D).} \end{cases} \quad (15)$$

As we consider large distances, we can perform a second-order Taylor expansion of $1/A(\mathbf{q})$ for $q\ell \ll 1$, which leads in the real space to a diffusion-type equation

$$-\frac{\ell^2}{d}\Delta I_D(\mathbf{r}) = I_B(\mathbf{r}), \quad (16)$$

where $d \in \{2,3\}$ is the space dimension. Solving Eq. (16) in a slab geometry, we obtain

$$
I_D(z) = \frac{I_0 d}{L + 2z_0} \left[(L + z_0 - z)\left(1 + \frac{z_0}{\ell}\right) \right.
$$
$$
\left. + (z + z_0)\left(1 - \frac{z_0}{\ell}\right)\exp\left(-\frac{L}{\ell}\right) \right] - I_0 d \exp\left(-\frac{z}{\ell}\right),
$$
(17)

where z_0 is the extrapolation length needed to account for the boundary conditions at the input and exit surfaces of the slab [26,27]. For a dilute index-matched slab, its expression is given by [27,28]

$$
z_0 = \begin{cases} \pi\ell/4 & \text{(2D)}, \\ 2\ell/3 & \text{(3D)}. \end{cases}
$$
(18)

This expression of the diffuse intensity I_D is *a priori* valid for distances z such that $z \gg \ell$, for which the diffusion approximation holds, but it surprisingly gives reasonably reliable results even for $z \lesssim \ell$. Adding the ballistic term, it also gives reliable results for the full average intensity
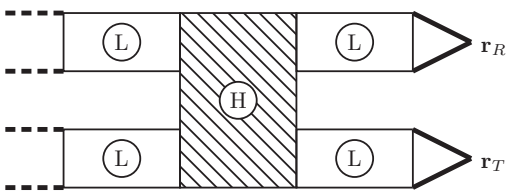
$$
\langle I(z) \rangle = I_B(z) + I_D(z),
$$
(19)

even for relatively small optical thicknesses.

2. Long-range C_2 contribution

The intensity correlation function is a fourth-order correlation in terms of field amplitude. Physically, a correlation is created when the two pairs of fields that constitute the intensities in the correlation function share a common history in the scattering process. Regarding C_2, the crossing occurs during the propagation of the intensities inside the system and is described by a complex object known as a Hikami vertex [29], and denoted by H in the following. The propagation of the intensity between the slab surfaces and the crossing is described by the ladder operator, denoted by L in the following. The expression of C_2 is given by [11,12,14,29]

$$
C_2(\mathbf{r}_R, \mathbf{r}_T) = \frac{1}{\langle I(\mathbf{r}_R)\rangle\langle I(\mathbf{r}_T)\rangle]} \int d\mathbf{r}_1 d\mathbf{r}_2 d\mathbf{r}_3 d\mathbf{r}_4
$$
$$
\times d\boldsymbol{\rho}_1 d\boldsymbol{\rho}_2 d\boldsymbol{\rho}_3 d\boldsymbol{\rho}_4 |\langle G(\mathbf{r}_R,\mathbf{r}_2)\rangle|^2 |\langle G(\mathbf{r}_T,\mathbf{r}_4)\rangle|^2
$$
$$
\times L(\mathbf{r}_2,\boldsymbol{\rho}_2)L(\mathbf{r}_4,\boldsymbol{\rho}_4)H(\boldsymbol{\rho}_1,\boldsymbol{\rho}_2,\boldsymbol{\rho}_3,\boldsymbol{\rho}_4)
$$
$$
\times L(\boldsymbol{\rho}_1,\mathbf{r}_1)L(\boldsymbol{\rho}_3,\mathbf{r}_3)|\langle E(\mathbf{r}_1)\rangle|^2 |\langle E(\mathbf{r}_3)\rangle|^2, \quad (20)
$$

which can be rewritten diagrammatically in the following form:
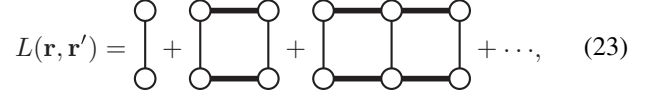
(21)

where the hatched box is the Hikami vertex and the other boxes are the ladder operators. Thick lines represent the average Green function, and thick dashed lines stand for the average electric field.

The ladder operator is defined as

$$
L(\mathbf{r},\mathbf{r}') = \gamma\delta(\mathbf{r} - \mathbf{r}') + \gamma \int |\langle G(\mathbf{r},\mathbf{r}'')\rangle|^2 L(\mathbf{r}'',\mathbf{r}')d\mathbf{r}'' \quad (22)
$$

and is represented diagrammatically as

where circles and thick horizontal solid lines represent scattering events and average Green functions, respectively, the top line standing for the field amplitude E and the bottom line for its complex conjugate E^*. Thin vertical solid lines link scattering events involving identical scatterers.

An analytical expression of the ladder operator can be obtained in the diffusive limit previously used for the computation of the average intensity. Making use of the translational invariance along the direction of the slab interface, the Fourier transform of the ladder operator with respect to transverse variables can be obtained from Eq. (22) and reads

$$
L(\mathbf{K},z,z') = \frac{d\,\gamma}{\ell^2 K} \frac{\sinh[K(z_< + z_0)]\sinh[K(L + z_0 - z_>)]}{\sinh[K(L + 2z_0)]},
$$
(24)

where $z_< = \min(z,z')$, $z_> = \max(z,z')$.

The Hikami box can also be calculated in the limit $k_0\ell \gg 1$, and its expression reduces to [11,12,14]

$$
H(\boldsymbol{\rho}_1,\boldsymbol{\rho}_2,\boldsymbol{\rho}_3,\boldsymbol{\rho}_4) = h \int \prod_{i=1}^{4} \delta(\boldsymbol{\rho} - \boldsymbol{\rho}_i)\nabla_{\boldsymbol{\rho}_2} \cdot \nabla_{\boldsymbol{\rho}_4} d\boldsymbol{\rho}, \quad (25)
$$

where

$$
h = \begin{cases} \ell^5/(16k_0^3) & \text{(2D)}, \\ \ell^5/(24\pi k_0^2) & \text{(3D)}. \end{cases}
$$
(26)

To have an explicit expression of C_2, we first compute the integrals involving $\mathbf{r}_1$ and $\mathbf{r}_3$ using

$$
\int L(\mathbf{r},\mathbf{r}')|\langle E(\mathbf{r}')\rangle|^2 d\mathbf{r}' = \gamma\langle I(\mathbf{r})\rangle.
$$
(27)

As we deal with large optical thicknesses, we can replace the average intensity by its diffuse component. Regarding the integrals involving $\mathbf{r}_2$ and $\mathbf{r}_4$, we assume that the ladder operators vary slowly at the scale of the scattering mean-free path ℓ. This amounts to replacing $\mathbf{r}_2$ by $\mathbf{r}_R$ and $\mathbf{r}_4$ by $\mathbf{r}_T$ in the ladder positions. We end up with an explicit expression of the

C_2 contribution to the correlation function, given by

$$C_2(\mathbf{r}_R,\mathbf{r}_T) = \frac{-I_0^2}{\langle I(\mathbf{r}_R)\rangle\langle I(\mathbf{r}_T)\rangle} \int_0^{+\infty} \frac{dq}{2q^2} F\left(\frac{q\,\Delta r}{L}\right)\left[\left\{q^2\left(1+\frac{2z_0}{L}+\frac{2z_0^2}{L^2}\right)+1\right\}\sinh(q)-q\cosh(q)\right]$$

$$\times \frac{L^2}{(L+2z_0)^2}\frac{\sinh(qz_0/L)^2}{\sinh[q(1+2z_0/L)]^2},$$

$$(28)$$

where

$$F\left(\frac{q\,\Delta r}{L}\right) = \left[1+\frac{z_0}{\ell}\right]^2 \times \begin{cases} \frac{16}{\pi k_0 \ell}\frac{\cos(q\,\Delta r/L)}{q} & \text{(2D)}, \\ \frac{27}{k_0^2 \ell L}\,J_0(q\,\Delta r/L) & \text{(3D)}. \end{cases} \quad (29)$$

The expression of the C_2 contribution to the reflection-transmission correlation function, together with its comparison to full numerical simulations, is the main result of this paper. The dependence of the amplitude on the system size L is approximatively L^{1-d}, with d the dimension of space. This shows that even at large optical thicknesses, a correlation subsists between the intensities measured in the transmitted and the reflected speckles and that this correlation is dominated by a contribution of the C_2 type.

It is important to keep in mind that this expression has been derived in the framework of the diffusion approximation (in particular, bulk average Green functions have been used). Its validity in the geometry considered here, where both reflected and transmitted intensities contribute, is checked by comparison to full numerical simulations in Fig. 2. It is interesting to note that the analytical and numerical calculations are in very good quantitative agreement, showing that the diffusion approximation, used to derive the analytical results, is very accurate even for an optical thickness $b = 7$ (that is not very large) and a geometry involving a reflected intensity (that always involves short scattering paths).

We have seen that C_2 decays algebraically with the system size L. Thus it is interesting to analyze the behavior of the full correlation function at smaller optical thicknesses, and in the crossover between the multiple- and single-scattering regimes. This problem can be addressed numerically by using the numerical method described previously in various scattering regimes and is the subject of the following section.

III. REFLECTION–TRANSMISSION CORRELATION AT SMALL OPTICAL THICKNESS

A. Numerical analysis

We consider a small optical thickness $b = 0.5$, corresponding to the single-scattering regime. The reflection-transmission intensity correlation function calculated numerically in this regime is shown in Fig. 3 (red solid line). The large oscillations observed on a scale on the order of the wavelength are not described by the C_2 contribution and are expected to be a signature of the short-range C_1 contribution. To check the validity of this assumption, we have to compute the C_1 contribution to the correlation function. At small optical thickness, a quantitative calculation would require to go beyond the diffusion approximation and to account properly for the boundary conditions [30]. Since our purpose in this section is only to support qualitatively the analysis of the general trends observed in the numerical simulations using

a simple model, we keep using the diffusion approximation to estimate the C_1 contribution.

B. C_1 contribution and specificity of the reflection-transmission configuration

In the scattering sequences picture, the C_1 correlation is created by interchanging the amplitudes between two independent ladders at the last scattering event. The C_1 contribution reads

$$C_1(\mathbf{r}_R,\mathbf{r}_T) = \frac{1}{\langle I(\mathbf{r}_R)\rangle\langle I(\mathbf{r}_T)\rangle}\int d\mathbf{r}_1 d\mathbf{r}_2 d\mathbf{r}_3 d\mathbf{r}_4$$

$$\times\langle G^*(\mathbf{r}_R,\mathbf{r}_4)\rangle\langle G(\mathbf{r}_T,\mathbf{r}_4)\rangle\langle G(\mathbf{r}_R,\mathbf{r}_2)\rangle\langle G^*(\mathbf{r}_T,\mathbf{r}_2)\rangle$$

$$\times L(\mathbf{r}_2,\mathbf{r}_1)L(\mathbf{r}_4,\mathbf{r}_3)|\langle E(\mathbf{r}_1)\rangle|^2|\langle E(\mathbf{r}_3)\rangle|^2. \quad (30)$$

In terms of diagrams, Eq. (30) can be rewritten as

$$C_1(\mathbf{r}_R,\mathbf{r}_T) = \qquad\qquad \mathbf{r}_T \quad \mathbf{r}_R. \quad (31)$$

In Eq. (30), the scattering of both pairs of fields from points $\mathbf{r}_1$ to $\mathbf{r}_2$ and from $\mathbf{r}_3$ to $\mathbf{r}_4$, respectively, is described by a ladder propagator. The mixing of amplitudes at the last scattering event is represented by four different average Green functions. The integrals in Eq. (30) can be factorized, leading to

$$C_1(\mathbf{r}_R,\mathbf{r}_T) = \frac{|B(\mathbf{r}_R,\mathbf{r}_T)|^2}{\langle I(\mathbf{r}_R)\rangle\langle I(\mathbf{r}_T)\rangle}, \quad (32)$$

FIG. 3. (Color online) Reflection–transmission intensity correlation C_{num} given by the numerical simulations (red solid line) and analytical correlation including all terms $C_1 + C_1' + C_2$ (blue dashed line). Single-scattering regime with $b = 0.5$ and $k_0\ell = 10$.

where

$$B(\mathbf{r}_R,\mathbf{r}_T) = \int \langle G(\mathbf{r}_R,\mathbf{r}_2)\rangle\langle G^*(\mathbf{r}_T,\mathbf{r}_2)\rangle$$
$$\times L(\mathbf{r}_2,\mathbf{r}_1)|\langle E(\mathbf{r}_1)\rangle|^2 d\mathbf{r}_1 d\mathbf{r}_2. \quad (33)$$

Equation (32) shows that C_1 is the square of the scattered field correlation function. Indeed, C_1 can also be seen as the correlation that would be observed for a field with Gaussian statistics, for which this factorization holds [31]. Starting from Eqs. (32) and (33), the usual way to derive the analytical expression of C_1 consists in replacing $\mathbf{r}_2$ by $\mathbf{r}_T$ (for a speckle computed in transmission) or $\mathbf{r}_2$ by $\mathbf{r}_R$ (for a speckle computed in reflection) in the ladder positions. In the reflection-transmission geometry, this simplification cannot be performed because the relative distance between the points $\mathbf{r}_T$ and $\mathbf{r}_R$ can be very large compared to the scattering mean free path ℓ. However, in order to get an explicit expression, we can make use of Eq. (27), which leads to

$$B(\mathbf{r}_R,\mathbf{r}_T) = \int \gamma\langle G(\mathbf{r}_R,\mathbf{r}_2)\rangle\langle G^*(\mathbf{r}_T,\mathbf{r}_2)\rangle\langle I(\mathbf{r}_2)\rangle d\mathbf{r}_2. \quad (34)$$

The integration over $\mathbf{r}_2$ is then performed using the residue theorem. (The details are given in Appendix.) This leads to

$$B(\mathbf{r}_R,\mathbf{r}_T) = \gamma I_0 \int \frac{\exp[-(ik'+k'')L - i\mathbf{K}\cdot\mathbf{\Delta r}]}{4(k'^2+k''^2)} \left[\frac{d\{(1+z_0/\ell)M_1 + (1-z_0/\ell)\exp(-L/\ell)M_2\}}{L+2z_0} - (d-1)M_3\right]\frac{d\mathbf{K}}{(2\pi)^{d-1}}, \quad (35)$$

where M_1, M_2, M_3, k', and k'' are given by Eqs. (A8)–(A10), and Eq. (A4), respectively. The last integral over $\mathbf{K}$ is performed numerically.

In the specific geometry considered here, another contribution has to be added in which the ballistic intensity contributes as one of the intensities involved in the correlation function [32]. Indeed, the ladder operator involves at least one scattering event and does not account for situations in which there is no scattering event before the field interchange. Such contributions to the correlation function can be important for small optical thicknesses where the ballistic contribution is not negligible. This leads to a correction to the C_1 correlation function, that we denote by C_1', and whose expression is

$$C_1'(\mathbf{r}_R,\mathbf{r}_T) = \frac{1}{\langle I(\mathbf{r}_R)\rangle\langle I(\mathbf{r}_T)\rangle}\langle E(\mathbf{r}_R)\rangle\langle E^*(\mathbf{r}_T)\rangle \int \langle G^*(\mathbf{r}_R,\mathbf{r}_2)\rangle\langle G(\mathbf{r}_T,\mathbf{r}_2)\rangle L(\mathbf{r}_2,\mathbf{r}_1)|\langle E(\mathbf{r}_1)\rangle|^2 d\mathbf{r}_1 d\mathbf{r}_2 + \text{c.c.} \quad (36)$$

In terms of diagrams, the above expression can be rewritten as

$$(37)$$
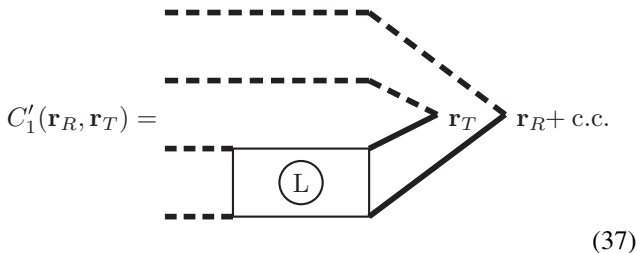
Making use of the quantity $B(\mathbf{r}_R,\mathbf{r}_T)$ defined in Eq. (33), we obtain

$$C_1'(\mathbf{r}_R,\mathbf{r}_T) = \frac{2\Re[\langle E^*(\mathbf{r}_R)\rangle\langle E(\mathbf{r}_T)\rangle B(\mathbf{r}_R,\mathbf{r}_T)]}{\langle I(\mathbf{r}_R)\rangle\langle I(\mathbf{r}_T)\rangle}. \quad (38)$$

It is important to note that the C_1' contribution introduced here, and that involves the average field, is not negligible compared to the usual C_1 contribution. This correction should be added to the C_1 contribution when the product of the ballistic fields $\langle E^*(\mathbf{r}_R)\rangle\langle E(\mathbf{r}_T)\rangle$ cannot be neglected, as in the reflection-transmission geometry at low optical thickness, or in the reflection-reflection geometry at any optical thickness. We can show from Eq. (35) that the C_1 and C_1' contributions to the correlation function decrease exponentially with the optical thickness $b = L/\ell$. This behavior explains why C_2 dominates at large optical thickness. But in the single-scattering regime, an important contribution of the $C_1 + C_1'$ term is observed. This is clearly seen in Fig. 3 (blue dashed line), in which the sum of the three contributions $C_1 + C_1' + C_2$ calculated analytically in the same two-dimensional geometry used for the numerical simulation is plotted. Qualitatively, the behavior observed in the numerical simulation is fairly reproduced by the analytical approach.

Moreover, since the $C_1 + C_1'$ contribution decays exponentially with the medium thickness L, a crossover is expected towards a regime dominated by C_2 when the optical thickness increases. This also shows that the reflection-transmission geometry studied here may be relevant to put forward experimentally the influence of the C_2 contribution. (In the pure reflection or transmission geometries, the C_1 contribution is always the leading contribution.)

IV. STATISTICAL DISTRIBUTION OF REFLECTED AND TRANSMITTED INTENSITIES

Analytical and numerical results at large optical thickness have shown that a correlation between reflected and transmitted intensities exists. Surprisingly, this correlation function takes negative values at around $\Delta r = 0$. Having $\langle \delta I(\mathbf{r}_R)\delta I(\mathbf{r}_T)\rangle < 0$ for $\Delta r = 0$ qualitatively suggests a high probability to have a bright (dark) spot in the transmitted speckle in coincidence with a dark (bright) spot in the reflected speckle. In order to address this question in more quantitative terms, we have studied the full statistical distribution of the intensities. More precisely, from the numerical simulations, we have extracted the statistical distributions of the product of the fluctuating part of the intensities at $\Delta r = 0$, defined as

$$P(\delta\tilde{I}_R\delta\tilde{I}_T) \equiv P\left[\frac{\delta I(\mathbf{r}_R)\delta I(\mathbf{r}_T)}{\langle I(\mathbf{r}_R)\rangle\langle I(\mathbf{r}_T)\rangle}\right], \quad (39)$$

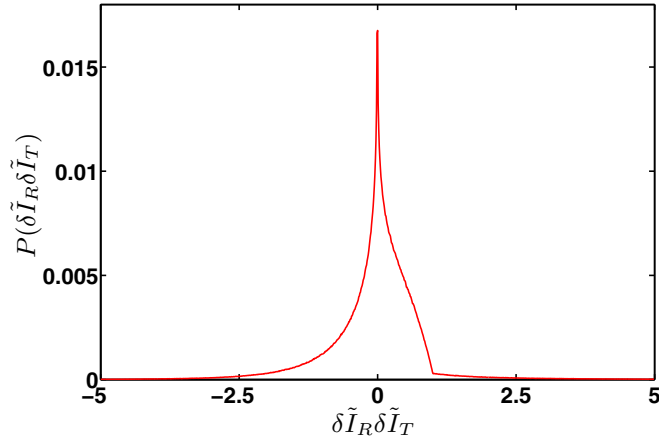whose average value is the intensity correlation $C(\mathbf{r}_R,\mathbf{r}_T)$ at $\Delta r = 0$.

FIG. 4. (Color online) Statistical distribution of the product of the normalized reflected–transmitted intensities $P(\delta \tilde{I}_R \delta \tilde{I}_T)$ at $\Delta r = 0$. Multiple-scattering regime with $b = 7$ and $k_0 \ell = 10$.

The statistical distribution $P(\delta \tilde{I}_R \delta \tilde{I}_T)$ obtained for $b = 7$ and $k_0 \ell = 10$ is shown in Fig. 4. The distribution exhibits an asymmetric shape, with a most likely value at $\delta I(\mathbf{r}_R) \delta I(\mathbf{r}_T) = 0$. Due to this asymmetric shape, the distribution cannot be simply characterized by its first moments. In particular, for $b = 7$ and $k_0 \ell = 10$, we find that the probability to have transmitted and reflected intensity fluctuations with opposite signs $P[\delta I(\mathbf{r}_R) \delta I(\mathbf{r}_T) < 0] = 0.47$, while we could have expected a much larger value (above 0.5) from a naive argument based on the negative sign of the correlation $C(\mathbf{r}_R, \mathbf{r}_T)$. Nevertheless, it is interesting to study statistics under some constraints. In particular, we have studied the probability of having $\delta I(\mathbf{r}_T) < 0$ (a spot in the transmitted speckle darker than the average intensity) under the assumption that $\delta I(\mathbf{r}_R) > n \langle I(\mathbf{r}_R) \rangle$, with $n \in \{0, 1, 2\}$ (i.e., for a coinciding spot in the reflected speckle with increasing brightness). The results are summarized in Table I. Interestingly, we find that the probability $P[\delta I(\mathbf{r}_T) < 0]$ increases substantially with the brightness of the reflected speckle spot, information that is not contained in the intensity correlation function. Consequently, if the reflected intensity in a speckle spot is large compared to the average reflected intensity, the transmitted intensity in the coinciding spot in the transmitted speckle is smaller than the average transmitted intensity with a large probability. This result may have implications in the context of light focusing

TABLE I. Probability of having $\delta I(\mathbf{r}_R) \delta I(\mathbf{r}_T) < 0$ (p), of having $\delta I(\mathbf{r}_T) < 0$ (q) at different optical thicknesses (b), and under some constraints ($\delta I(\mathbf{r}_R) > n \langle I(\mathbf{r}_R) \rangle$ with $n \in \{0, 1, 2\}$) for $\Delta r = 0$ and $k_0 \ell = 10$.

				q	
b	p	q	$\delta I(\mathbf{r}_R) > 0$	$\delta I(\mathbf{r}_R) > \langle I(\mathbf{r}_R) \rangle$	$\delta I(\mathbf{r}_R) > 2\langle I(\mathbf{r}_R) \rangle$
0.5	0.48	0.57	0.57	0.62	0.67
1	0.50	0.61	0.64	0.69	0.74
2	0.47	0.64	0.64	0.67	0.69
4	0.47	0.65	0.65	0.67	0.67
7	0.47	0.66	0.66	0.67	0.67

through opaque scattering media by wave-front shaping. Indeed, maximizing the intensity in a reflected speckle spot might, with a high probability, lead to a minimization of the intensity in the corresponding transmitted spot. A precise study with optimized wave fronts (beyond plane-wave illumination) is left for future work.

V. CONCLUSION

In summary, we have studied analytically and numerically the spatial correlation between intensities measured in the reflected and transmitted speckles generated by a slab of disordered scattering medium. We have demonstrated the existence of a reflection-transmission correlation. At large optical thicknesses, the spatial correlation persists and is dominated by the C_2 contribution, thus exhibiting a long-range behavior. Interestingly, this correlation takes negative values. At small optical thicknesses, the correlation is dominated by a C_1-type contribution, which contains the usual C_1 term and an additional term C_1' involving the ballistic intensity.

The statistical connection between transmitted and reflected speckles might be of interest for wave-front shaping methods used to focus and image through scattering media. Since for practical implementations only the reflected speckle can be measured and controlled, a knowledge of the probability to get a bright (dark) spot in the transmitted speckle in coincidence with a dark (bright) spot in the optimized reflected speckle could be a great advantage. As a first step towards this goal, we have studied the statistical distributions of reflected and transmitted intensities and have identified situations in which the probability of coincidence of bright and dark spots on opposite sides of the medium is high.

Finally, a refinement of the analytical model would be beneficial to deal with optical thicknesses for which the diffusion approximation fails to give quantitative results. One possibility could be to develop a semianalytical approach (coupling analytical expressions and numerical calculations) based on the radiative transfer equation [33] that accurately described short and long scattering paths [34].

ACKNOWLEDGMENTS

APPENDIX: ANALYTICAL CALCULATION OF B

In the reflection-transmission configuration, the usual approximation used to calculate C_1 breaks. Indeed in transmission-transmission or in reflection-reflection one usually manages to separate in Eq. (33) integrals over $\mathbf{r}_2$ and $\mathbf{r}_1$ because of the small distance between the two points where we compute the correlation. In our configuration, because of the large distance between these two points, we have to explicitly calculate $B(\mathbf{r}_R, \mathbf{r}_T)$.

Using the symmetry of the problem, taking the Fourier transform of the two Green functions over their transverse coordinates, we simplify Eq. (33) in the following way:

$$B(\mathbf{r}_R,\mathbf{r}_T) = \int \gamma \langle I(z_2) \rangle \langle G(z_2,\mathbf{K}) \rangle \langle G^*(z_2 - L,\mathbf{K}) \rangle$$

$$\times \exp[-i\mathbf{K} \cdot \boldsymbol{\Delta}\mathbf{r}] dz_2 \frac{d\mathbf{K}}{(2\pi)^{d-1}}, \quad \text{(A1)}$$

where z_2 is the depth at which the two fields separate. To calculate the expression of the Green function in this mixed domain, one can see that

$$\langle G(z_2,\mathbf{K}) \rangle = \int \langle G(k,\mathbf{K}) \rangle \exp[ikz_2] \frac{dk}{2\pi}$$

$$= \int \frac{\exp[ikz_2]}{k^2 + K^2 - k_{\text{eff}}^2} \frac{dk}{2\pi}. \quad \text{(A2)}$$

Equation (A2) can be calculated using the residue theorem using the fact that $k_{\text{eff}}^2 = k_0^2 + ik_0/\ell$ and noting that

$$\frac{1}{k^2 + K^2 - k_{\text{eff}}^2} = \frac{1}{(k - k_+)(k + k_+)}, \quad \text{(A3)}$$

where

$$k_+ = \sqrt{k_0^2 + ik_0/\ell - K^2} = k' + ik'' \quad \text{(A4)}$$

is the pole with a positive imaginary part (i.e., $k'' > 0$). Thus Eq. (A2) can be calculated with the residue theorem by integrating over a contour composed of the real axis and an upper half circle, the radius of which tends to infinity. We obtain that

$$\langle G(z_2,\mathbf{K}) \rangle = \frac{i}{2k_+} \exp(ik_+ z_2). \quad \text{(A5)}$$

Following the same steps we can show that

$$\langle G^*(z_2 - L,\mathbf{K}) \rangle = \frac{-i}{2k_+^*} \exp[ik_+^*(z_2 - L)], \quad \text{(A6)}$$

leading to

$$B(\mathbf{r}_R,\mathbf{r}_T) = \gamma \int \langle I(z_2) \rangle \frac{\exp[2ik'z_2]}{4(k'^2 + k''^2)} \exp[-ik_+^* L]$$

$$\times \exp[-i\mathbf{K} \cdot \boldsymbol{\Delta}\mathbf{r}] dz_2 \frac{d\mathbf{K}}{(2\pi)^{d-1}}. \quad \text{(A7)}$$

Using the expression of the average intensity, we have to perform three integrations, denoted respectively by M_1, M_2, and M_3:

$$M_1 = \int_0^L (L + z_0 - z_2) \exp[2ik'z_2] dz_2$$

$$= \frac{1 + 2ik'(L + z_0) - \exp[2ik'L](1 + 2ik'z_0)}{4k'^2}, \quad \text{(A8)}$$

$$M_2 = \int_0^L (z_0 + z_2) \exp[2ik'z_2] dz_2$$

$$= \frac{2ik'z_0 - 1 + \exp[2ik'L][1 - 2ik'(L + z_0)]}{4k'^2}, \quad \text{(A9)}$$

$$M_3 = \int_0^L \exp\left(-\frac{z_2}{\ell}\right) \exp[2ik'z_2] dz_2$$

$$= \ell \frac{1 - \exp[2ik'L] \exp[-L/\ell]}{1 - 2ik'\ell}. \quad \text{(A10)}$$

With these expressions, we can rewrite the final expression of $B(\mathbf{r}_R,\mathbf{r}_T)$ as a Fourier transform given by Eq. (35).

[1] *Waves and Imaging Through Complex Media*, edited by P. Sebbah (Kluwer Academic, Dordrecht, 2001).

[2] P. Sheng, *Introduction to Wave Scattering, Localization and Mesoscopic Phenomena* (Academic Press, New York, 1995).

[3] I. M. Vellekoop and A. P. Mosk, Opt. Lett. **32**, 2309 (2007).

[4] S. M. Popoff, G. Lerosey, R. Carminati, M. Fink, A. C. Boccara, and S. Gigan, Phys. Rev. Lett. **104**, 100601 (2010).

[5] I. M. Vellekoop, A. Lagendijk, and A. P. Mosk, Nat. Photonics **4**, 320 (2010).

[6] S. Popoff, G. Lerosey, M. Fink, A. C. Boccara, and S. Gigan, Nat. Commun. **1**, 81 (2010).

[7] A. P. Mosk, A. Lagendijk, G. Lerosey, and M. Fink, Nat. Photonics **6**, 283 (2012).

[8] I. M. Vellekoop and C. M. Aegerter, Opt. Lett. **35**, 1245 (2010).

[9] J. Bertolotti, E. G. van Putten, C. Blum, A. Lagendijk, W. L. Vos, and A. P. Mosk, Nature (London) **491**, 232 (2012).

[10] O. Katz, P. Heidmann, M. Fink, and S. Gigan, Nat. Photonics **8**, 784 (2014).

[11] R. Berkovits and S. Feng, Phys. Rep. **238**, 135 (1994).

[12] M. C. W. van Rossum and T. M. Nieuwenhuizen, Rev. Mod. Phys. **71**, 313 (1999).

[13] *Wave Scattering in Complex Media: From Theory to Applications*, edited by B. van Tiggelen and S. Skipetrov, NATO Sciences Series II Vol. 107 (Kluwer, Dordrecht, 2003).

[14] E. Akkermans and G. Montambaux, *Mesoscopic Physics of Electrons and Photons* (Cambridge University Press, Cambridge, UK, 2007).

[15] C. W. J. Beenakker, Rev. Mod. Phys. **69**, 731 (1997).

[16] B. Shapiro, Phys. Rev. Lett. **57**, 2168 (1986).

[17] B. Shapiro, Phys. Rev. Lett. **83**, 4733 (1999).

[18] A. Cazé, R. Pierrat, and R. Carminati, Phys. Rev. A **82**, 043823 (2010).

[19] R. Sarma, A. Yamilov, P. Neupane, B. Shapiro, and H. Cao, Phys. Rev. B **90**, 014203 (2014).

[20] R. Carminati, G. Cwilich, L. S. Froufe-Pérez, and J. J. Sáenz, Phys. Rev. A **91**, 023807 (2015).

[21] J. J. Sáenz, L. S. Froufe-Pérez, and A. García-Martín, in *Wave Scattering in Complex Media: From Theory to Applications*, edited by B. van Tiggelen and S. Skipetrov, NATO Science Series II Vol. 107 (Kluwer, Dordrecht, 2003), p. 175.

[22] L. S. Froufe-Pérez, A. García-Martín, G. Cwilich, and J. J. Sáenz, Physica A **386**, 625 (2007).

[23] S. Feng, C. Kane, P. A. Lee, and A. D. Stone, Phys. Rev. Lett. **61**, 834 (1988).

[24] M. J. Stephen and G. Cwilich, Phys. Rev. Lett. **59**, 285 (1987).

[25] M. Lax, Phys. Rev. **85**, 621 (1952).

[26] K. M. Case and P. F. Zweifel, *Linear Transport Theory* (Addison-Wesley, Reading, MA, 1967).

[27] A. Ishimaru, *Wave Propagation and Scattering in Random Media*, The IEEE/OUP Series on Electromagnetic Wave Theory (IEEE Press & OUP, New York/Oxford, UK, 1997).

[28] Y. Lai, S.-K. Cheung, and Z.-Q. Zhang, Phys. Rev. E **72**, 036606 (2005).

[29] S. Hikami, Phys. Rev. B **24**, 2671 (1981).

[30] I. Freund and D. Eliyahu, Phys. Rev. A **45**, 6133 (1992).

[31] P. Sebbah, B. Hu, A. Z. Genack, R. Pnini, and B. Shapiro, Phys. Rev. Lett. **88**, 123901 (2002).

[32] D. B. Rogozkin and M. Y. Cherkasov, Phys. Rev. B **51**, 12256 (1995).

[33] S. Chandrasekhar, *Radiative Transfer* (Dover, New York, 1950).

[34] R. Elaloufi, R. Carminati, and J. J. Greffet, J. Opt. Soc. Am. A **21**, 1430 (2004).